

FIGURE 3. Comparison of GRB 050326 with the Amati (right) and Ghirlanda (left) relations [6, 7]. The thick solid curves (black and grey) show the position of GRB 050326 as its redshift varies in the interval $0.1 < z < 10$. The Ghirlanda track is actually a boundary (as the horizontal arrows indicate), since we can only infer a lower limit to the beaming-corrected energy at each redshift. Filled circles and squares indicate the GRBs which define the above two relations, plotted as straight solid lines (together with their 1-, 2- and 3- σ contours: long-dashed, dot-dashed and dotted lines, respectively). Data were taken from [6, 8]. Grey diamonds indicate the intersection of the GRB 050326 tracks with the 3- σ contours of the Amati and Ghirlanda relations. These points thus define the 3- σ redshift ranges for which GRB 050326 was consistent with the two relations. In the two GRB 050326 tracks, the region $1.5 < z < 8$ (indicated by the X-ray data) is shown in black, bound by asterisks.

3. Galama, T.J., & Wijers, R.A.M.J. 2001, *Apj*, 549, L209
4. Stratta, G., Fiore, F., Antonelli, L.A., Piro, L., & De Pasquale, M. 2004, *Apj*, 608, 846
5. Campana, S., Romano, P., Covino, S., et al. 2005b, *A&A*, in press (astro-ph/0511750)
6. Ghirlanda, G., Ghisellini, G., & Lazzati, D. 2004, *Apj*, 616, 331
7. Amati, L., Frontera, F., Tavani, M., et al. 2002, *A&A*, 390, 81
8. Ghirlanda, G., Ghisellini, G., Lazzati, D., & Firmani, C. 2005, Il nuovo cimento, in press (astro-ph/0504184)

GRB 050117: Simultaneous Gamma-ray and X-ray Observations with the Swift Satellite

J.E. Hill^{1,2}, D. C. Morris³, T. Sakamoto¹, G. Sato⁴, D.N. Burrows³, L. Angelini^{1,5}, C. Pagani^{3,6}, A. Moretti⁶, A.F. Abbey⁷, S. Barthelmy¹, A.P. Beardmore⁸, V.V. Biryukov⁹, S. Campana⁵, M. Capalbi¹⁰, G. Cusumano¹¹, P. Giommi¹⁰, M.A. Ibrahimov¹², J.A. Kennea³, S. Kobayashi^{3,13}, K. Ioka^{3,13}, C. Markwardt¹⁴, P. Meszaros³, P.T. O'Brien⁸, J.P. Osborne⁸, A.S. Pozanenko¹⁴, M. Peiri¹⁶, V.V. Rumyantsev¹⁵, P. Schady¹⁶, D.A. Sharapov¹², G. Tagliaferri⁵, B. Zhang¹⁷, G. Chincarini^{6,18}, N. Gehrels¹, A. Wells^{3,7}, J.A. Nousek³

¹NASA/GSFC, Greenbelt, MD 20771, USA.

²USRA, Columbia, MD, 21044, USA.

³Department of Astronomy & Astrophysics, Penn State University, University Park, PA 16802, USA.

⁴ISAS/Japan Aerospace Exploration Agency, Kanagawa, 229-8510, Japan.

⁵The Johns Hopkins University, Baltimore, MD 21218, USA

⁶INAF-Osservatorio Astronomico di Brera, 23807 Merate, Italy.

⁷Space Research Centre, University of Leicester, Leicester LE1 7RH, UK.

⁸Department of Physics and Astronomy, University of Leicester, Leicester LE1 7RH, UK.

⁹Crimean Laboratory of Sternberg Astronomical Institute, Moscow University, Russia

¹⁰ASI Science Data Center, 00044 Frascati, Italy.

¹¹INAF - Istituto di Astrofisica Spaziale e Fisica Cosmica Sezione di Palermo, 90146 Palermo, Italy.

¹²Ugugh Beg Astronomical Institute, Tashkent, 700052, Uzbekistan.

¹³Center for Gravitational Wave Physics, Pennsylvania State University, University Park, PA 16802, USA.

¹⁴Space Research Institute, Moscow 117810, Russia.

¹⁵Crimean Astrophysical Observatory, Ukraine

¹⁶Midland Space Science Laboratory, Holnbury St. Mary, Dorling, Sarrey, UK.

¹⁷Department of Physics, University of Nevada, Las Vegas, NV 89154, USA

¹⁸Universit  degli studi di Milano-Bicocca, Dipartimento di Fisica, I-20126 Milan, Italy

Abstract. The Swift Gamma-Ray Burst Explorer performed its first autonomous, X-ray follow-up to a newly detected GRB on 2005 January 17, within 193 seconds of the burst trigger by the Swift Burst Alert Telescope. While the burst was still in progress, the X-ray Telescope obtained a position and an image for an un-catalogued X-ray source; simultaneous with the gamma-ray observation. The XRT observed flux during the prompt emission was 1.1×10^{-8} ergs cm^{-2} in the 0.5-10 keV energy band. The emission in the X-ray band decreased by three orders of magnitude within 700 seconds, following the prompt emission. This is found to be consistent with the gamma-ray decay when extrapolated into the XRT energy band. During the following 6.3 hours, the XRT observed the afterglow in an automated sequence for an additional 947 seconds, until the burst became fully obscured by the Earth limb. A faint, extremely slowly decaying afterglow, $\alpha \sim 0.21$, was detected. Finally, a break in the lightcurve occurred and the flux decayed with $\alpha \sim 1.2$. The X-ray position triggered many follow-up observations: no optical afterglow could be confirmed, although a candidate was identified 3 arcsecs from the XRT position.

Keywords: gamma rays - bursts - general; gamma-rays, X-rays - individual (GRB 050117)

On 2005 January 17 at 12:52:36.037 UT, the *Swift* Burst Alert Telescope triggered and called GRB 050117 (Sakamoto et al. GCN 2952). For the first time, *Swift* responded autonomously to the BAT triggered burst, pointing the XRT at the GRB while the burst was still in progress, and allowing simultaneous gamma-ray and X-ray flux measurements of the prompt emission and follow up observations of the afterglow. The measurements of the burst, which lasted 220 seconds, is multi-peaked. The XRT was on target and obtained a refined position and an image within 193 seconds of the BAT detection (Figure 1). The XRT detected the GRB at the end of the burst on-set, measuring source position of RA(J2000)= $23^{\text{h}} 53^{\text{m}} 53.0^{\text{s}}$ Dec(J2000)= $+65^{\circ} 56' 19.8''$ (Hill et al. GCN 2955) and an absorbed flux of $1.1 \pm 0.3 \times 10^{-8}$ ergs $\text{cm}^{-2} \text{s}^{-1}$ in the 0.5-10 keV band. A faint afterglow was detected by the XRT during the subsequent orbits. The UVOT activation was not complete at the time of these observations and therefore it remained in non-observing state throughout. No radio or optical afterglow was detected by the ground based follow-up observations.

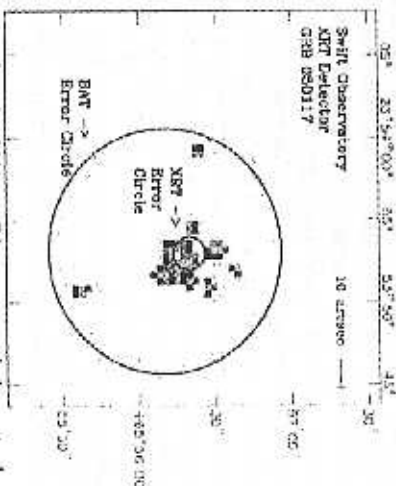


FIGURE 1. XRT Image showing the 90% confidence error circle centered on the onboard position, overlaid on a non-normal spacecraft configuration and the BAT 90% confidence error circle from ground processing.

Gamma-ray Analysis

The time-averaged spectral fit over the 15-150 keV energy band gave a photon index of 1.1 ± 0.2 and an E_{peak} of 123 ± 50 keV. The burst total energy fluence was $9.3 \pm 0.2 \times 10^6$ ergs cm^{-2} in the 15-150 keV band in 220 seconds with more than one third of the fluence in the 100-150 keV band. The peak photon flux of 2.47 ± 0.17 ph $\text{cm}^{-2} \text{s}^{-1}$ (integrated for one second from 15-150 keV using the best fit model of a simple power-law) occurred 227.22 seconds after the trigger.

XRT Analysis

The X-ray lightcurve is shown in Figure 2. The X-ray data indicate a decrease in flux of almost three orders of magnitude between the prompt emission at $t=190$ seconds and

the afterglow at $t=900$ seconds. The decay becomes significantly flatter over the following ~6 hours and then becomes steeper again sometime later in order to be undetected 43 days after the burst.

A photo-absorbed power law spectral fit to the prompt emission ($t=193$ seconds) using a Galactic absorption column yields a photon index of 2.3 ± 0.5 . Fitting the same model to the summed data from the afterglow ($t=900$ seconds - 6.6 hours) yields a photon index of 2.0 ± 1.1 .

For the X-ray data we assume a spectrum of the form $F(t, \nu) \propto (t-t_0)^{\alpha} \nu^{\beta}$, where β is the spectral index and $\alpha = 1 - \text{photon index}$, yielding a spectral index of -1.3 ± 0.5 and -1.0 ± 1.1 for the prompt and follow-up observations, respectively.

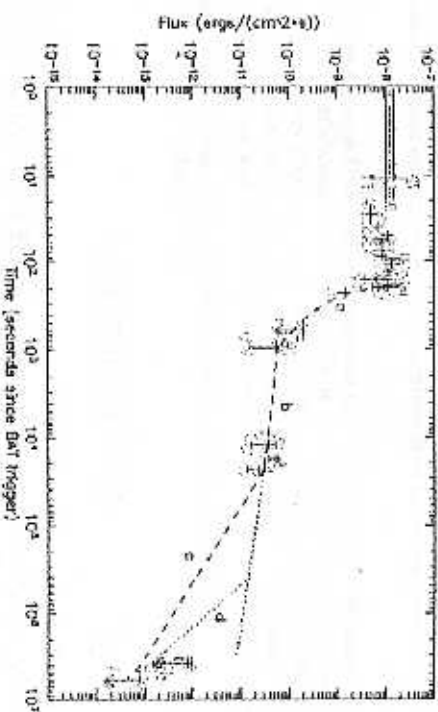


FIGURE 2. GRB 050117 lightcurve (absorbed fluxes): The BAT (blue) lightcurve using the spectral fits for each time bin and extrapolating the 15-100 keV flux into the 0.5-10 keV band and the XRT (red) lightcurve (0.5-10 keV), showing the upper limits for the observations at more than 43 days after the burst. a) A power law fit assuming high latitude emission from the internal shock where $t_{\text{peak}}=187$ seconds, $\alpha < -1.2$; b) A power law fit to the afterglow decay with energy input from refreshed shocks assuming a t_0 -trigger time, $\alpha = -0.2 \pm 0.2$; c) Continuation of the afterglow decay assuming a break in the lightcurve at $t=6.6$ hours, t_0 -trigger time, $\alpha = -1.2$; d) Extrapolation of $\alpha = -2$ from $t=43$ days, showing the latest expected time of the break in the lightcurve at ~4.5 days (t_0 -trigger time).

The XRT and extrapolated BAT fluxes obtained from the simultaneous XRT and BAT observations (Figure 2) are well within the 90% confidence limits. If we consider that the multiple peaks in the BAT lightcurve are attributed to internal shocks from the collision of the faster expanding shells with slower shells in front, then it is reasonable to assume that the X-ray flux at this time was also produced by an internal shock collision.

The minimum expected emission following the peak from the internal shock is the high latitude emission from the curvature effect (Kumar & Panaitescu, 2000). The angular spreading time scale determines the decay timescale, and consequently the width of an internal shock peak, Δt . Therefore, t_0 of the internal shock is, $t_{\text{peak}}=187$ seconds. Due to the non-detection of gamma-ray flux between $t=300$ seconds and $t=915$ seconds we can assume that the X-ray flux after 900 seconds is dominated by the decaying afterglow and therefore we can use the XRT flux measurement at 900 seconds as an upper limit on the contribution from the decaying internal shock at this time.

This provides a constraint on the temporal decay of the internal shock of $\alpha < -1.1$. In the context of high latitude emission from the internal shock, where $\alpha = \beta - 2$, and taking the photon index of 2.3 ± 0.5 into consideration, a decay of -3.3 ± 0.5 would be expected. This is within the constraints of the observation, where $\alpha < -1.1$.

Following the end of the prompt emission, the lightcurve enters a shallower decay phase where, for the following 6.3 hours, there is very little decay in flux. The 90% confidence upper limit for the decay index is -0.5, but the best fit to the data is shallower than this; $\alpha = -0.21 \pm 0.3$. A second break in the power law is implied by the steep decay between the data points at 23 ksec and the upper limit at 68 days. In order for the source to be undetected 68 days after the burst, the flux must decay with $\alpha < -1.2$ if the break occurred immediately after the last detection. If the break occurred later or the flux is significantly less than the upper limit, then the decay could be steeper.

The afterglow due to the collision with the ambient medium may have started while the internal shock emission was still in progress, although the sample rate is too low to confirm this. The emission from the afterglow appears to be enhanced by the additional input of energy from lagging shells of ejected material. This burst was long and multi-wavelengthed, and therefore if the later shells were slow moving with a modest Lorentz factor, energy would be injected into the afterglow as each shell collides into the external medium. This would cause re-brightening super-imposed on the nominal afterglow decay and could explain the flatter than expected decay between 900 seconds and 6.6 hours. The lightcurve is not well sampled and so bumps, which may be expected from re-brightening, cannot be discerned from the lightcurve. The refreshed shock energy injection continues until at least five hours after the burst. Some time between five hours and 4.5 days after the burst trigger, the refreshed shocks ceased and the lightcurve turned over to a steeper decay rate of $\alpha < -1.2$ corresponding to the expected afterglow decay, thus the burst was below the XRT detection threshold at $t = 68$ days.

To date, there have only been three other observations by *Swift* with simultaneous gamma-ray and X-ray detections. The observations of GRB 050117 demonstrate the unique capability of *Swift* to observe both the burst and the afterglow in the X-ray regime.

ACKNOWLEDGEMENTS

This work is supported at Penn State by NASA contract NAS5-00136; at the University of Leicester by the Particle Physics and Astronomy Research Council on grant number PP/A/Z/S/2003/00507; and at OAB by funding from ASI on grant number PR/03/9/04. We gratefully acknowledge the contributions of dozens of members of the *Swift* team at PSU, University of Leicester, OAB, GSFC, ASDC and our subcontractors, who helped make this Observatory possible and to the Flight Operations Team for their dedication and support.

REFERENCES

- Cassano, G. 2005, *The Astrophysical Journal*, in press
Lightheart, G. et al. 2005, *Nature*, Vol. 436, Issue 7053, 985
Kumar, P. and Panaitescu, A. 2000, *The Astrophysical Journal*, 541, L51
Hill, J.E., et al. 2005, GCN 2955
Sakamoto, T., et al. 2005, GCN 2952

Rapid GRB Afterglow Response With SARA

K. V. Garrimella^{*}, A. L. Homewood^{*}, D. H. Hartmann^{*}, C. Riddle^{*},
S. Fuller^{*}, A. Manning^{*}, T. McIntyre^{*}, G. Henson[†]

^{*}Clemson University, Department of Physics & Astronomy, and SARA Observatory, Clemson, SC 29634
[†]Department of Physics and Astronomy, East Tennessee State University, Johnson City, TN 37614

Abstract. The Clemson GRB Follow-Up program utilizes the SARA 0.9m telescope to observe optical afterglows of Gamma Ray Bursts. SARA is not yet robotic; it operates under direct and Target-of-Opportunity (ToO) interrupt modes. To facilitate rapid response and timely reporting of data analysis results, we developed a software suite that operates in two phases: first, to notify observers of a burst and assist in data collection, and second, to quickly analyze the images.

Keywords: Rapid Response, Perl, website, automation, gamma-ray bursts.
PACS: 95.75.-z, 95.75.Mn, 95.75.Rs

1. INTRODUCTION

Swift notifies other observatories of GRBs through email and socket messages called "GCN Notices". Socket communication is preferable to email alerts for automated systems, since information comes in smaller chunks with header information indicating the type of message. Messages arrive more quickly than emails, and a client-side script can more easily filter these socket messages into reasonable commands for a telescope. We utilize remote, human-controlled access to the SARA 0.9m telescope (not yet) operational under a fully scripted schedule). Therefore the notices are more important for notifying the team rather than directly instructing the telescope to respond. For this purpose, the email method is sufficient. The format of the emails facilitates parsing through a regular expressions engine in any preferred language. We have written such a notification tool in Perl, a language well suited in an environment where string manipulations are numerous. This tool notifies group members by email and text-messages to phones. In addition, the tool also extracts key information from the Notices and assembles a page on a website with burst-specific data (coordinate history, finding charts, rise and set times, weather information, and in the case of a false particle trigger, retractions). Rapid data analysis becomes necessary to quickly return relevant information to the community. We have written scripts for standard image reduction sequences with minimum user-input.